

Journal Pre-proofs

Synthesis of novel feruloyl dipeptides with proapoptotic potential against different cancer cell lines

Abdelaaty Hamed, Marcel Frese, Menna Elgaafary, Tatiana Syrovets, Norbert Sewald, Thomas Simmet, Mohamed Shaaban

PII: S0045-2068(19)31922-4
DOI: <https://doi.org/10.1016/j.bioorg.2020.103678>
Reference: YBIOO 103678

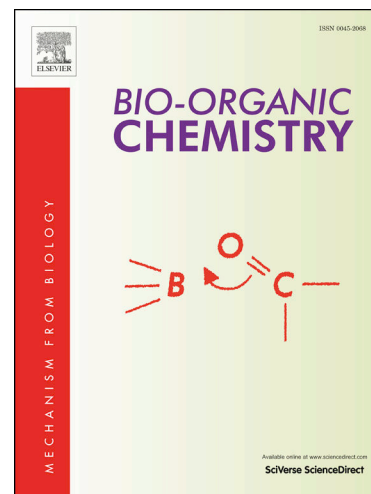
To appear in: *Bioorganic Chemistry*

Received Date: 11 November 2019
Revised Date: 30 January 2020
Accepted Date: 19 February 2020

Please cite this article as: A. Hamed, M. Frese, M. Elgaafary, T. Syrovets, N. Sewald, T. Simmet, M. Shaaban, Synthesis of novel feruloyl dipeptides with proapoptotic potential against different cancer cell lines, *Bioorganic Chemistry* (2020), doi: <https://doi.org/10.1016/j.bioorg.2020.103678>

This is a PDF file of an article that has undergone enhancements after acceptance, such as the addition of a cover page and metadata, and formatting for readability, but it is not yet the definitive version of record. This version will undergo additional copyediting, typesetting and review before it is published in its final form, but we are providing this version to give early visibility of the article. Please note that, during the production process, errors may be discovered which could affect the content, and all legal disclaimers that apply to the journal pertain.

© 2020 Published by Elsevier Inc.



Synthesis of novel feruloyl dipeptides with proapoptotic potential against different cancer cell lines

Abdelaaty Hamed^{1,2*}, Marcel Frese¹, Menna Elgaafary^{3,4}, Tatiana Syrovets³, Norbert Sewald¹, Thomas Simmet^{3*} and Mohamed Shaaban^{1,5*}

¹Organic and Bioorganic Chemistry, Faculty of Chemistry, Bielefeld University, D-33501 Bielefeld, Germany

²Chemistry Department, Faculty of Science, Al-Azhar University, Nasr City-Cairo 11884, Egypt

³Institute of Pharmacology of Natural Products and Clinical Pharmacology, Ulm University, Ulm, D-89081, Germany

⁴Department of Pharmacognosy, College of Pharmacy, Cairo University, Cairo, 11562, Egypt

⁵Chemistry of Natural Compounds Department, Pharmaceutical and Drug Industries Research Division, National Research Centre, El-Buhouth St. 33, Dokki-Cairo 12622, Egypt

* Correspondence: abdohamed481@yahoo.com (Abdelaaty Hamed); thomas.simmet@uni-ulm.de (Thomas Simmet), mshaaba@gmail.com (Mohamed Shaaban)

Abstract:

In this study, a series of novel *N*-feruloyl dipeptides (**10-17**) have been synthesized through the coupling of *N*-feruloyl amino acids (**6-9**) with glycine/alanine methyl ester hydrochloride. Structures of the peptides were assigned using 1D and 2D NMR and HRESIMS. According to initial *in vitro* cytotoxic screening against the cervix carcinoma cell line KB-3-1, aromatic dipeptides (**12**, **13**, **16**, **17**) were the most potent ones among all tested feruloyl dipeptides. Accordingly, these peptides were further intensively investigated as potential anticancer agents against a panel of ten cancer cell lines from different tissue origin. Based on that, compound **17** showed the strongest cytotoxic efficiency towards the whole panel of tested cell lines with IC₅₀ values from 2.1 to 7.9 μM. By contrast, the dipeptides **12**, **13** and **16** showed moderate to weak cytotoxicity (IC₅₀ 16.1-28.3 or > 30, 5.7-21.9 and 3.9-21.2 or ≥ 30 μM, respectively). Mechanistically, compound **17** induced a strong dissipation of the mitochondrial transmembrane potential and an early activation of caspase 3/7 in the triple-negative MDA-MB-231 breast cancer cell line. In an *in vivo* model, compound **17** inhibited growth, proliferation and induced apoptosis in MDA-MB-231 xenografted onto the chick chorioallantoic membrane. All the synthesized

compounds were also tested against a set of pathogenic bacterial strains, displaying no potential activity.

Keywords: Feruloyl-dipeptides; *In vitro* cytotoxicity; Caspase-3/7; Mitochondrial potential; Triple negative breast cancer; CAM xenografts

1. Introduction

Being the second leading cause of mortality, cancer represents the major public health concern in the United States and many other parts of the world [1]. Particularly, breast, lung, cervical, liver, prostate and pancreatic cancers are the most frequent causes of death worldwide with cancer death rates depending strongly on gross national product (GNP) per capita and health-care expenditures [2].

Breast cancer is the most frequently diagnosed cancer type and the leading cause of cancer-related mortality in females worldwide. The high mortality from breast cancer is consistently due to tumor metastases [2]. Triple-negative breast cancers (TNBC) are among the most aggressive and deadly breast cancer subtypes with a high risk of tumor relapse. TNBC affects more frequently younger premenopausal women and metastasizes to critical visceral organs [3-5]. Therefore, there is worldwide interest in the design of new approaches in the management and treatment of this life-threatening disease either through exploration of new natural products or synthetic chemistry.

Ferulic acid is a naturally abundant plant's phenolic compound [6-11], which, due to its low toxicity even in high doses [12], has recently been approved as an antioxidant in food additives [13,14]. Additional therapeutic claims of FA encompassing anticarcinogenic [15], antidiabetic [16], hepatoprotective [17-19], antimicrobial, anti-inflammatory [20-22], anticholesterolemic [23], neuroprotective [24], UV protective [25] and radioprotective [26] effects motivated us to synthesize new *N*-feruloyl-dipeptide conjugates as an approach to explore new promising anticancer agents of low side effects and toxicity. Thereby, we have created novel ferulic acid derivatives with increased lipophilicity and membrane penetration, hence, maximizing their bioavailability and therapeutic value.

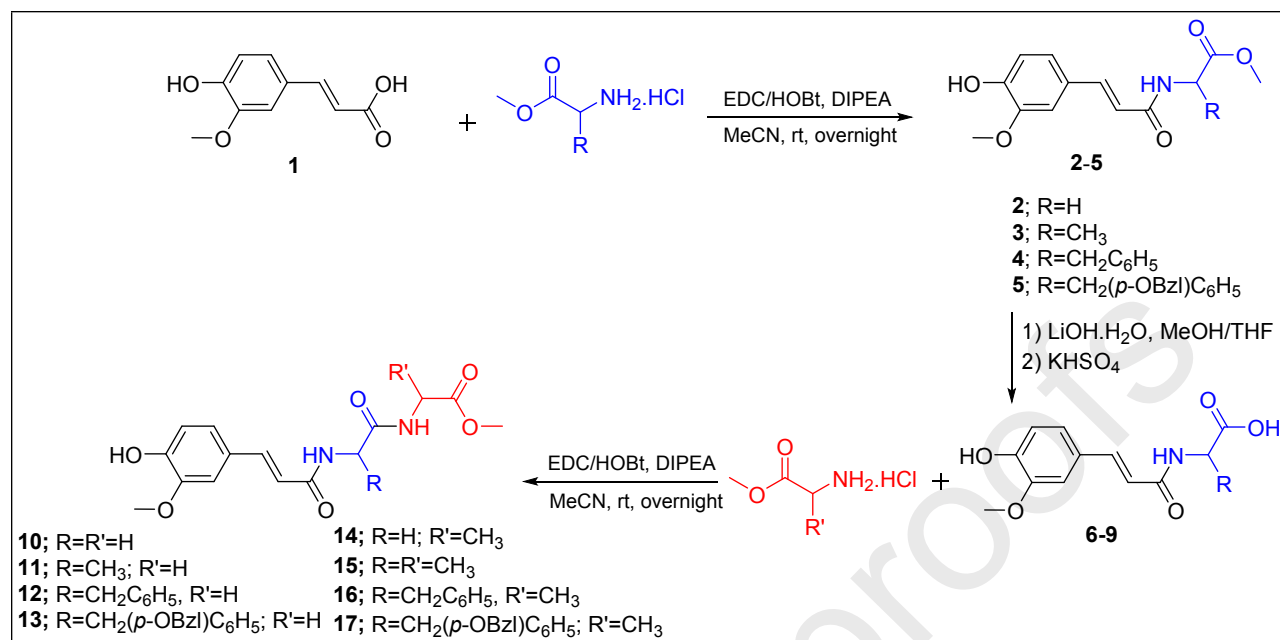
2. Results and discussion

2.1. Chemistry

As illustrated in Scheme 1, the formation of amide linkage between ferulic acid and *C*-protected amino acids was achieved according to recently reported literature [27] to produce *N*-feruloyl amino acid methyl esters (**2-5**) of colorless solids appearance. Chemical structures of the latter were assigned on the basis of their physicochemical properties and spectroscopic data (NMR, ESI-MS) and comparison with corresponding references [28-30].

Based on ESI-MS, the molecular weights of compounds **2-5** were determined as 265, 279, 355, and 461 Da, respectively. The ¹H NMR of **2-5** displayed ¹H of an amide group between 8.38-8.41 ppm, and their amide and ester carbonyls were assigned in ¹³C NMR spectra in the range of 165.7-166.4 and 171.0-173.7 ppm, respectively, confirming the amide linkage between ferulic acid and corresponding amino acid methyl esters. Further details are delineated in the experimental section; hence structures **2-5** were definitely determined.

The formation of the free *N*-feruloyl amino acids derivatives **6-9** was achieved by alkaline hydrolysis of **2-5** using lithium hydroxide and subsequent acidification with potassium hydrogen sulphate [27]. Structures of the de-esterified compounds **6-9** were established by NMR and ESI-MS data. Their molecular weights (251, 265, 341, and 447 Da) were deduced to be of 14 amu less than the original esters (**2-5**) [30-32] corresponding to the conversion of -COOCH₃ to -COOH. Meanwhile, their ¹H NMR shifts are most likely retained, except the missed methoxy groups signals, in addition, the amide and hydroxyl ¹H protons appeared between δ 8.20-8.25 ppm and δ 9.45-9.46 ppm, respectively. The ¹³C NMR spectra showed the amide carbonyls between 165.6-166.2 ppm, meanwhile, those of the free carboxylic acids are between δ 171.9-174.7 ppm.



Scheme 1: Synthetic scheme of feruloyl amino acid methyl esters (**2-5**), corresponding acids (**6-9**) and dipeptides (**10-17**)

A subsequent individual coupling of the free amino acid derivatives **6-9** with glycine and alanine methyl esters hydrochloride, following the same procedure applied for compounds **2-5** [15], afforded the new *N*-feruloyl dipeptide methyl esters **10-13** and **14-17**, respectively, as colorless solids. Structures of compounds **10-17** were established on the basis of 1D and 2D-NMR, and HR-ESI-MS data (see the Supplementary Data).

Detailed structural discussion of *N*-feruloyl-L-tyrosyl(OBzl)glycine methyl ester (**13**) based on spectroscopic analysis is taken herein as representative example of the dipeptides **10-17**. The molecular weight of **13** was deduced as 518 Da based on positive and negative modes of ESI-MS, delivering the molecular formula C₂₉H₃₀N₂O₇ of 16 double bond equivalents (DBE). ¹H NMR spectrum demonstrated a broad singlet of phenolic OH (δ 9.46); triplet and doublet of peptidic 1NH were shown at δ 8.53 and 8.16 ppm, respectively. Ten signals integrated for fourteen protons were shown in the aromatic/olefinic region being for 1,2,4-tri-substituted, 1,4-di-substituted and mono-substituted aromatic residues, in addition to one double bond, four signals in the oxygenated region integrated for 9H representing CH, ABX-CH₂ (δ 3.02 and 2.75) and 2CH₃. Twenty-five resonating signals integrated for 29 carbons were assigned according to ¹³C/HSQC, which were classified into 3 C=O of ester and/or amide (δ 172.5, 170.7 and 165.6); three phenolic *sp*² carbons, three non-oxygenated *sp*² C_q, 14 *sp*² methines, O-CH₂, N-CH₂, N-CH, 2 OCH₃ and 3 *Sp*³-CH₂.

Further assignment of structure **13** was accomplished by 2D-NMR spectral data (**Figure 1**). H,H COSY cross peaks between H-5/H-6, H-2/H-3 confirmed the ferulic acid fragment (**A**). Similarly, the tyrosine (OBzl) fragment (**B**) was fixed through the COSY cross peaks between NH-1'/H-2'/H-3', H-5'/H-6', H-8'/H-9', and H-13'/H-14'/H-15'/H-16'/H-17'. The structure of the third fragment (**C**) was deduced as well through the COSY correlations between NH-1'' and H-2'' and HMBC correlations from H-2'' and H₃-4'' towards C-3''. The direct linkage between **A** and **B** was deduced by the shown ³J HMBC correlation from H-2' to C-1, the third fragment **C** was subsequently attached to **B** through the ³J HMBC correlation from H-2'' to C-10'.

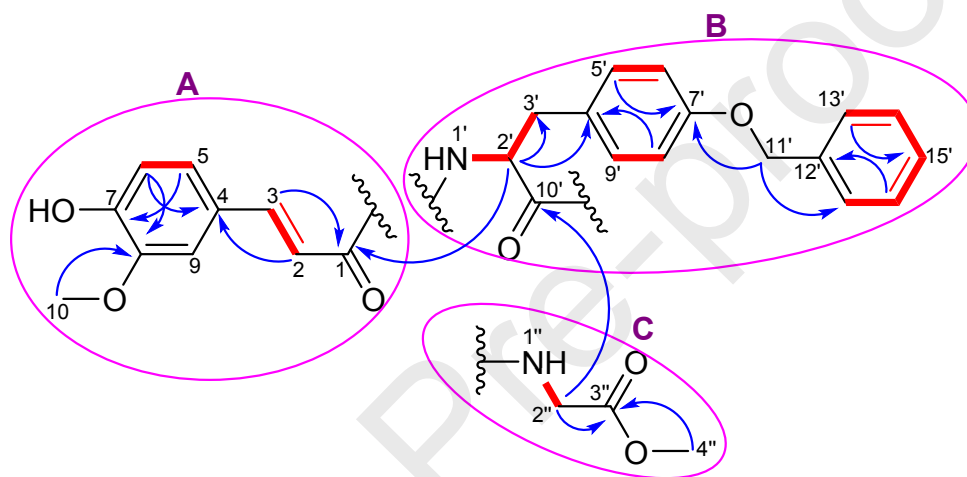


Figure 1. COSY (—) and key HMBC (↷) connectivities of compound **13**.

2.2. Evaluation of Biological Activities

2.2.1. Antibacterial Activity

Using agar diffusion testing method [33] with a concentration of 0.5 mg/ml, the synthesized compounds were tested against a set of pathogenic Gram-positive (*Bacillus subtilis* DSMZ 704, *Micrococcus luteus* DSMZ 1605, *Staphylococcus warneri* DSMZ 20036) and Gram-negative (*Escherichia coli* DSMZ 1058, *Pseudomonas. agarici* DSMZ 11810) bacterial strains in comparison with gentamycin as reference. However, the compounds exhibited no potentiality as antibacterial agents.

2.2.2. In Vitro Cytotoxic Activity

The newly obtained *N*-feruloyldipeptide methyl esters (**10-17**), *N*-feruloylamino acid methyl ester **5**, the previously reported *N*-feruloylamino acid methyl esters (**2-4**) [28-30] and ferulic acid (**1**) were screened for their *in vitro* cytotoxic activity against the KB-3-1 cervix carcinoma cell line. The results indicated that coupling of ferulic acid with aromatic amino acid moieties produced the most promising activities. In particular, *N*-feruloyl-L-tyrosyl(OBzl)glycine methyl ester (**13**), *N*-feruloyl-L-phenylalanyl-L-alanine methyl ester (**16**) and *N*-feruloyl-L-tyrosyl(OBzl)-L-alanine methyl ester (**17**) showed the highest activity with IC₅₀ values of 57, 45 and 17 μM, respectively **Table 1**. On the other hand, feruloyl derivatives with aliphatic amino residues showed the least or no activity at all.

Table 1: *In-vitro* cytotoxicity of the synthesized compounds **2-5**, **10-17** against KB-3-1 cell line:

Compound	IC ₅₀ (μM)	Compound	IC ₅₀ (μM)
1	-	12	>100
2	-	13	57
3	-	14	>100
4	-	15	>100
5	>100	16	45
10	-	17	17
11	-		

Based on the aforementioned interesting cytotoxic profile of *N*-feruloyl dipeptide methyl esters **12**, **13**, **16** and **17**, they were further evaluated by using an XTT cell viability kit and a panel of ten human cancer cell lines originating from six different types of solid tumors in comparison with paclitaxel as a positive control. The response parameter expressed as IC₅₀ values of the tested compounds against the above-mentioned cancer cell lines are listed in **Table 2**. As expected and previously shown [34], we found, that ferulic acid exhibited no obvious cytotoxicity towards the tested cancer cell panel at the concentration range tested. By contrast, the synthesized ferulic acid dipeptide derivatives (**12**, **13**, **16** and **17**) showed a more pronounced cytotoxicity towards all tested cancer cell lines (**Figure 2**, **Table 2**). In addition, the potency order of cytotoxic activity of the synthesized derivatives against the human cancer cell lines used can be arranged as **17** > **16** ≅ **13** > **12**. Compound **12** displayed the weakest cytotoxic activity with IC₅₀ values in the range of 16.1-28.3 or > 30.0 μM, whereas compounds **13** and **16** showed moderate cytotoxicity with IC₅₀ values in the range of 5.7-21.9 μM and 3.9-21.2 or ≥ 30.0 μM, respectively. Compound **17** revealed

the highest *in vitro* cytotoxicity (IC₅₀ range 2.1-7.9 μM) towards all tested cancer cell lines. The most bioactive ferulic acid peptide derivative, **17**, inhibited the proliferation and cell viability of breast cancer cells, the TNBC MDA-MB-231, MDA-MB-453, CAL-148 and CAL-51 with IC₅₀ values of 4.6, 2.2, 2.1 and 2.8 μM, respectively, and of the triple-positive (TPBC) MCF7 with IC₅₀ of 2.2 μM. In addition, compound **17** exhibited cytotoxic activity against MIA PaCa-2 pancreatic carcinoma cells, DU 145 androgen-insensitive prostate carcinoma cells, HeLa cervical carcinoma cells, Hep G2 hepatocellular carcinoma cells and A549 pulmonary adenocarcinoma cells with IC₅₀ values of 2.5, 4.0, 4.7, 5.9, and 7.9 μM, respectively.

The high cytotoxic activity of **17** toward different human cancer cell lines prompted us to further investigate the molecular mechanism of cancer cell death induced by it. TNBC are among the most aggressive and deadly breast cancer subtypes [3-5]. For that reason, the MDA-MB-231 TNBC breast cancer cell line was selected as a representative cell line to perform such studies.

Table 2. Toxicity of *N*-feruloyl dipeptide methyl esters **12**, **13**, **16** and **17** against a panel of solid cancer cell lines

Tissue	Cell lines	Compound, IC ₅₀ , 48 h					
		μM				nM	
		12	13	16	17	Ferulic acid	Paclitaxel
Breast TPBC	MCF7	>30	16.2	22	2.2	> 30	*
Breast TNBC	MDA-MB-231	>30	20.8	18.4	4.6	> 30	-
Breast TNBC	MDA-MB-453	28.3	5.7	5.3	2.2	> 30	48 nM
Breast TNBC	CAL-51	20.3	7.8	6.5	2.8	> 30	41 nM
Breast TNBC	CAL-148	16.1	5.8	3.9	2.1	> 30	-
Liver	Hep G2	> 30	19.4	21.2	5.9	> 30	-
Cervix	HeLa	> 30	14	17.1	4.7	> 30	4.9 nM
Lung	A549	> 30	21.9	≥ 30	7.9	> 30	-
Pancreas	MIA PaCa-2	22.5	5.9	6.6	2.5	> 30	7.2 nM
Prostate	DU 145	> 30	7.1	19.2	4	> 30	6.5 nM

TPBC (triple-positive breast cancer), TNBC (triple-negative breast cancer), - (not done), *(cannot be properly estimated)

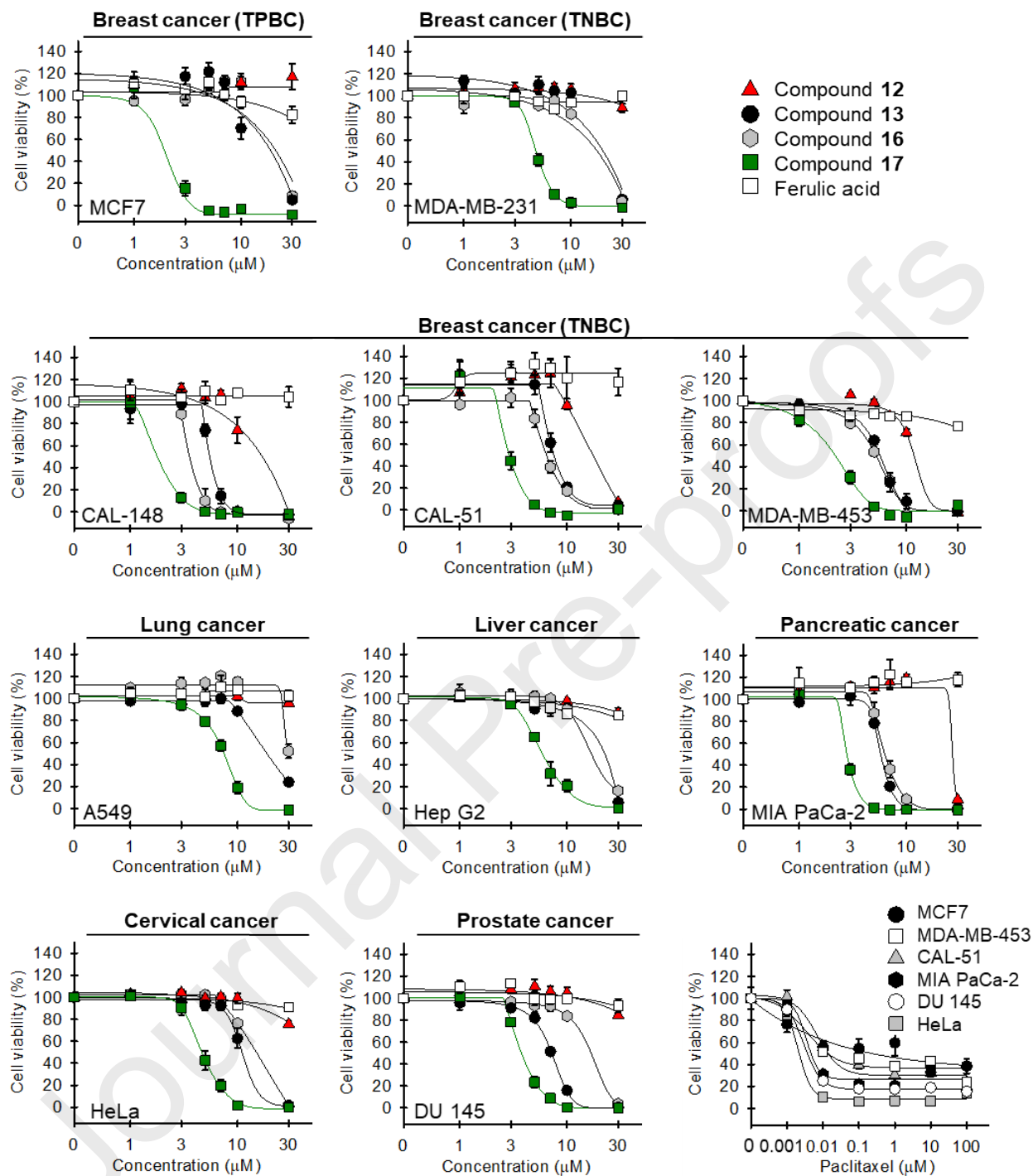


Figure 2. Cytotoxic activity of compounds **12,13,16** and **17** against a panel of 10 solid human cancer cell lines. Compound **17** shows the strongest cytotoxic activity. The cancer cell lines were treated with various concentrations of compounds **12, 13, 16, 17**, or the parental ferulic acid for 48 h. Cell viability was analyzed by a XTT cell viability assay. All data are mean \pm SEM, n = 3. Paclitaxel served as control.

2.2.3. Induction of Mitochondrial Dysfunction

Mitochondria act as central check point of apoptosis by integrating death signals originating from both, the extrinsic and intrinsic apoptotic signaling pathways [35]. To delineate the importance of mitochondria in compound **17**-induced cancer cell death, the mitochondrial membrane integrity was analyzed by using the lipophilic cationic JC-1 dye that exhibits potential-dependent accumulation in the mitochondria. The dye specifically enters and accumulates inside the negatively-charged energized mitochondria in a potential-dependent manner to form red fluorescent J-aggregates, whereas from damaged mitochondria, it is released into the cytoplasm, where it can be detected as green fluorescent monomers. Among the analyzed synthesized ferulic acid derivatives, only compound **17**, at the used concentration of 10 μM , induced a strong collapse of mitochondrial membrane potential in TNBC MDA-MB-231 cells after 24 h (**Figure 3**). This mitochondrial dissipation is characterized by a red-to-green fluorescence emission shift and an increase in the percentages of cells with deenergized mitochondria to about 68% similar to those observed by the potent mitochondrial oxidative phosphorylation uncoupler, FCCP (**Figure 3**).

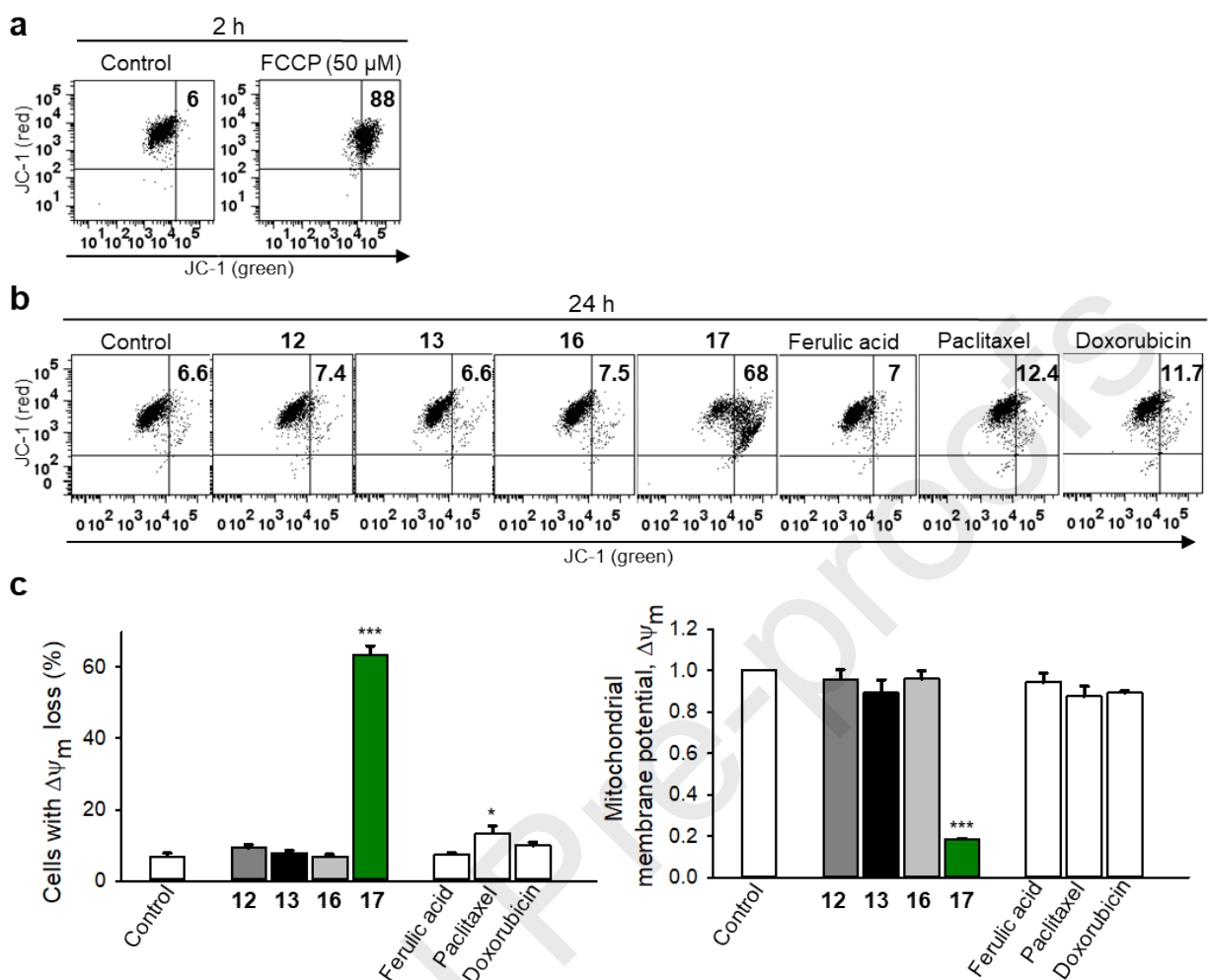


Figure 3. Compound 17 affects the mitochondrial integrity in the triple-negative MDA-MB-231 breast cancer cell line. (a) MDA-MB-231 cells treated with the respiratory uncoupler, FCCP (50 μM) for 2 h were used as positive control. (b) MDA-MB-231 cells were treated with either ferulic acid, its synthesized derivatives at concentrations of 10 μM , or paclitaxel (100 nM), or doxorubicin (100 nM) for 24 h. The mitochondrial membrane potential was analyzed flow cytometrically by using JC-1 dye. Representative dot plots are shown. Figures (upper right squares of the panels) show the percentages of cells with the loss of mitochondrial membrane potential ($\Delta\Psi_m$). $\Delta\Psi_m$ was measured as red/green JC-1 fluorescence intensity ratio. (c) Graphs show the percentages of MDA-MB-231 cells with depolarized mitochondria and the loss of $\Delta\Psi_m$ in treated cells. Statistical analysis was performed by using the Newman-Keuls test. All data are mean \pm SEM, n = 3, * p < 0.05, *** p < 0.001 vs control.

2.2.4. Activation of Executioner Caspase 3/7

Mitochondria play an integral role in the activation of the caspase cascade in the intrinsic apoptotic signaling pathway [35]. Caspases 3 and 7 are the best characterized executioner caspases that when cleaved activate a large set of substrates to produce the morphological and biochemical features associated with apoptosis [36]. Treatment of the TNBC MDA-MB-231 cells with compound **17** (10 and 30 μM) for 24 h induced a strong activation of caspase 3/7 followed by a relative decrease with increasing the incubation time (Figure 4).

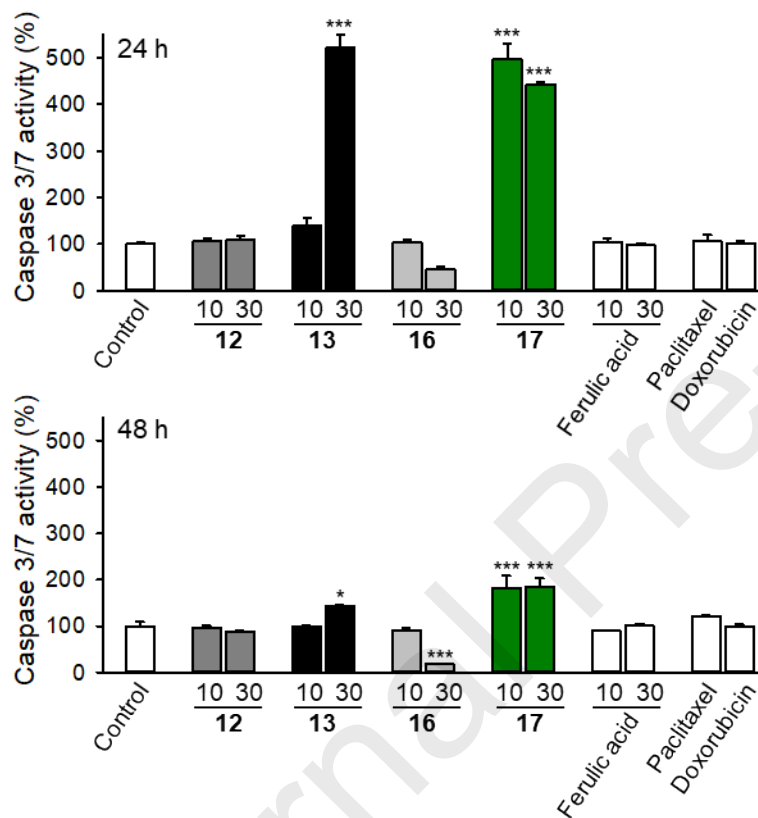


Figure 4. Compound **17** induces activation of caspase 3/7 in the triple-negative MDA-MB-231 breast cancer cell line. MDA-MB-231 cells were treated with either ferulic acid, or its synthesized derivatives at concentrations of 10 and 30 μM , paclitaxel (100 nM), or doxorubicin (100 nM) for 24 and 48 h, and the activity of caspase 3/7 was assessed using a Caspase-Glo® 3/7 activity kit according to the manufacturer's instructions. Graphs show the percentage of caspase 3/7 activation in treated cells relative to the control. All data are mean \pm SEM, $n = 3$, * $p < 0.05$, *** $p < 0.001$ vs control.

2.2.5. *In Vivo* Antitumor Efficacy in Human Triple-Negative MDA-MB-231 Xenografts

The *in vitro* antitumor efficacies of different synthesized ferulic acid derivatives were further assessed in an *in vivo* model using MDA-MB-231 xenografts on the chorioallantoic membrane of

fertilized chick eggs (CAM). Immunohistochemical analysis revealed that all synthesized ferulic acid derivatives inhibited the expression of the nuclear antigen Ki-67, used as a marker for growth and proliferation of the tumor xenografts. Moreover, they induced DNA strand breaks, a sign of terminal apoptosis, in the highly aggressive MDA-MB-231 xenografts (**Figure 5**). In particular, compound **17** exhibited the strongest antitumour activity in the established human tumor xenograft model, in terms of inhibition of tumor growth, proliferation and the induction of apoptosis (**Figure 5**). Upon examination of the embryos, neither embryonic death nor any signs of systemic toxicity could be detected with compound **17** treatment indicating low systemic toxicity.

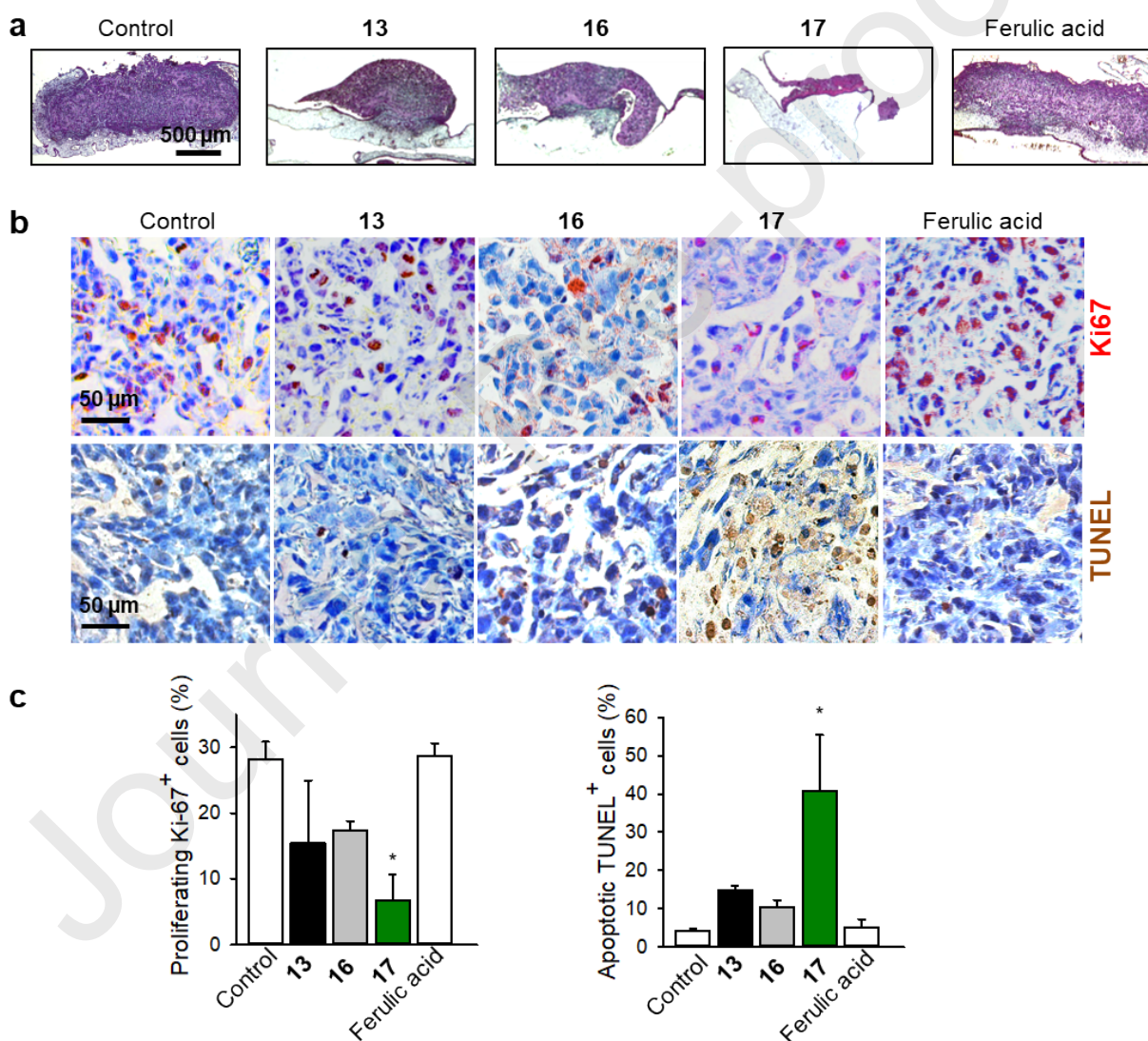


Figure 5. Compound **17** induces apoptosis and inhibits growth of the triple-negative MDA-MB-231 breast cancer xenografts *in vivo*. MDA-MB-231 cells were grafted onto the chorioallantoic membrane (CAM) of fertilized chick

eggs. Next day, the tumors were topically treated with compounds **13**, **16**, and **17** at the concentration of 10 μ M for 3 consecutive days. (a) Representative pictures are shown. Hematoxylin and eosin staining (HE) after histological preparation, original magnification 50x. (b) Upper panel: immunohistochemical analysis of tumor cell proliferation using nuclear Ki-67 antigen (proliferation marker, dark violet stain within nuclei). Nuclei were counterstained with hematoxylin (blue). Original magnification 200x. Lower panel: TUNEL staining (TdT, dark brown) for the detection of cells with fragmented DNA as apoptosis marker. Original magnification 200x. (c) Graphs show quantification of tumor cell proliferation and apoptosis. Statistical analysis was performed by using the Newman-Keuls test, $n = 3 - 4$, $*p < 0.05$ vs control.

3. Experimental

3.1. Chemistry

Melting points were determined on a BÜCHI Melting Point B-540 apparatus (BÜCHI Germany). NMR spectra (^1H NMR, ^{13}C NMR, COSY, HMQC, and HMBC) were measured on Bruker Avance DRX 500 MHz (125 MHz for ^{13}C NMR) spectrometer (Bruker, USA) with tetramethylsilane as internal standard. Chemical shifts were reported relative to residual solvent peaks ($[\text{D}_6]$ dimethyl sulphoxide (DMSO): ^1H : 2.50 ppm, ^{13}C : 39.5 ppm). ESI mass spectra were recorded using an ion trap mass spectrometer equipped with a standard ESI/APCI source. Samples were introduced by direct infusion with a syringe pump. Nitrogen served both as the nebulizer gas and the dry gas. Nitrogen was generated by a nitrogen generator. Helium served as cooling gas for the ion trap and collision gas for MSn experiments (Bruker Daltonik GmbH, Bremen, Germany). Starting materials, reagents, and solvents were obtained from Sigma-Aldrich (St. Louis, MO, USA) and used without further purification. The purity of the synthesized compounds was investigated by thin layer chromatography (TLC), performed on Merck precoated silica gel 60 F254 aluminum sheets with solvent mixture of dichloromethane-methanol as eluent. Spots were visualized under an ultraviolet (UV) lamp at 254 and 366 nm then staining with anisaldehyde/ H_2SO_4 reagent.

3.1.1. General procedure for synthesis of *N*-feruloylamino acid methyl esters (2-5)

Ferulic acid (1 eq), amino acid methyl ester hydrochloride (1 eq), 1-hydroxybenzotriazole (HOBT) (1.2 eq) and 1-ethyl-3-(3-dimethylaminopropyl)carbodiimide hydrochloride (EDC-HCl) (1.2 eq) in dry acetonitrile (6 ml) were stirred at 0 $^\circ\text{C}$ for five minutes, then *N,N*-diisopropylethylamine (DIPEA) (1.2 eq) was added dropwise. The reaction mixture was stirred overnight at room temperature. The solvent was removed under reduced pressure and the residue was dissolved in

dichloromethane (DCM) and washed by deionized water, sodium hydrogen carbonate and 1M hydrochloric acid. The DCM layer was then dried over MgSO_4 and the solvent was removed under reduced pressure to produce *N*-feruloylamino acid methyl esters **2-5** as white solids. Spectroscopic data of **2-5** are listed below.

3.1.1.1. *N*-feruloylglycine methyl ester (**2**)

White solid (yield % = 91 %); mp 112-113 °C. ^1H NMR ($\text{DMSO-}d_6$, 500 MHz): δ = 9.49 (s, OH), 8.38 (t, J = 6.0 Hz, 1H, amide-NH), 7.36 (d, J = 15.7 Hz, 1H), 7.16 (d, J = 2.0 Hz, 1H), 7.03 (dd, J = 8.2, 2.0 Hz, 1H), 6.81 (d, J = 8.1, Hz, 1H), 6.54 (d, J = 15.7 Hz, 1H), 3.97 (d, J = 5.9 Hz, 2H), 3.82 (s, 3H), 3.65 (s, 3H); ^{13}C NMR ($\text{DMSO-}d_6$, 125 MHz): δ = 171.0 ($\underline{\text{COOMe}}$), 166.4 (CONH), 148.9, 148.3, 140.3, 126.6, 122.2, 118.5, 116.1, 111.3, 56.0, 52.2, 41.2; (+)-ESIMS m/z 266 ($[\text{M} + \text{H}]^+$), 288 ($[\text{M} + \text{Na}]^+$, 100).

3.1.1.2. *N*-feruloyl-*L*-alanine methyl ester (**3**)

White solid (yield % = 76 %); mp 117-118 °C. ^1H NMR ($\text{DMSO-}d_6$, 500 MHz): δ = 9.49 (s, OH), 8.38 (d, J = 7.1 Hz, 1H, amide-NH), 7.34 (d, J = 15.8 Hz, 1H), 7.14 (d, J = 2.0 Hz, 1H), 7.01 (dd, J = 8.2, 2.0 Hz, 1H), 6.80 (d, J = 8.1, Hz, 1H), 6.50 (d, J = 15.7 Hz, 1H), 4.39 (p, J = 7.2 Hz, 1H), 3.81 (s, 3H), 3.64 (s, 3H), 1.33 (d, J = 7.3 Hz, 3H); ^{13}C NMR ($\text{DMSO-}d_6$, 125 MHz): δ = 173.7 ($\underline{\text{COOMe}}$), 165.7 (CONH), 148.9, 148.3, 140.2, 126.7, 122.1, 118.6, 116.1, 111.2, 56.0, 52.3, 48.1, 17.6; (+)-ESIMS m/z 302 $[\text{M} + \text{Na}]^+$; (-)-ESIMS m/z 278 $[\text{M-H}]^-$.

3.1.1.3. *N*-feruloyl-*L*-phenylalanine methyl ester (**4**)

White solid (yield % = 68 %); mp 107-108 °C. ^1H NMR ($\text{DMSO-}d_6$, 500 MHz): δ = 9.49 (s, OH), 8.41 (d, J = 7.8 Hz, 1H, amide-NH), 7.35-7.18 (m, 6H), 7.12 (d, J = 1.9 Hz, 1H), 6.99 (dd, J = 8.1, 1.9 Hz, 1H), 6.80 (d, J = 8.0, Hz, 1H), 6.50 (d, J = 15.8 Hz, 1H), 4.62 (ddd, J = 9.7, 7.6, 5.3 Hz, 1H), 3.81 (s, 3H), 3.62 (s, 3H), 3.09 (dd, J = 13.8, 5.4 Hz, 1H), 2.96 (dd, J = 13.8, 9.3, 1H); ^{13}C NMR ($\text{DMSO-}d_6$, 125 MHz): δ = 172.7 ($\underline{\text{COOMe}}$), 165.9 (CONH), 148.9, 148.3, 140.4, 137.7, 129.5, 128.7, 127.0, 126.6, 122.3, 118.4, 116.1, 111.1, 56.0, 54.2, 52.3, 37.3; (+)-ESIMS m/z 378 $[\text{M} + \text{Na}]^+$; (-)-ESIMS m/z 354 $[\text{M-H}]^-$.

3.1.1.4. *N*-feruloyl-*L*-tyrosine(OBzl) methyl ester (**5**)

White solid (yield % = 70 %); mp 122-123 °C. ¹H NMR (DMSO-*d*₆, 500 MHz): δ = 9.48 (s, OH), 8.37 (d, *J* = 7.8 Hz, 1H, amide-NH), 7.43 (d, *J* = 7.8 Hz, 2H), 7.38 (d, *J* = 7.7 Hz, 2H), 7.31 (m, 2H), 7.16 (d, *J* = 8.6 Hz, 2H), 7.12 (d, *J* = 2.0 Hz, 1H), 6.99 (dd, *J* = 8.2, 1.9 Hz, 1H), 6.93 (d, *J* = 8.6 Hz, 2H), 6.80 (d, *J* = 8.1 Hz, 1H), 6.51 (d, *J* = 15.7 Hz, 2H), 5.06 (s, 2H), 4.56 (ddd, *J* = 9.7, 7.7, 5.4 Hz, 1H), 3.81 (s, 3H), 3.62 (s, 3H), 3.02 (dd, *J* = 13.9, 5.4 Hz, 1H), 2.89 (dd, *J* = 13.9, 9.2, 1H); ¹³C NMR (DMSO-*d*₆, 125 MHz): δ = 172.7 (COOMe), 165.9 (CONH), 157.5, 148.9, 148.3, 140.3, 137.6, 130.5, 129.8, 128.9, 128.2, 128.1, 126.6, 122.2, 118.5, 116.1, 115.0, 111.1, 69.6, 56.0, 54.4, 52.3, 36.5; (+)-ESIMS *m/z* 484 [M + Na]⁺; (-)-ESIMS *m/z* 460 [M-H]⁻.

3.1.2. General procedure for synthesis of *N*-feruloylamino acids (**6-9**)

N-feruloylamino acid methyl esters (**2-5**) (1 eq) were dissolved in MeOH/THF (1:1) then a solution of LiOH.H₂O (2.5 eq) in H₂O was added dropwise. The reaction mixture was stirred at room temperature for 1 h and then the solvents were removed under reduced pressure. The residual aqueous phase was acidified by adding solid KHSO₄ (pH = 4 - 5) and re-extracted with AcOEt twice. The combined extracts were dried over MgSO₄ and the solvent was removed under reduced pressure to yield *N*-feruloylamino acids (**6-9**) as white solids. Spectroscopic data of these compounds are listed below.

3.1.2.1. *N*-feruloyl-glycine (**6**)

White solid (yield % = 86 %); mp 216-217 °C. ¹H NMR (DMSO-*d*₆, 500 MHz): δ = 12.54 (s, OH), 9.46 (s, COOH), 8.25 (t, *J* = 5.9 Hz, 1H, amide-NH), 7.35 (d, *J* = 15.7 Hz, 1H), 7.16 (d, *J* = 2.0 Hz, 1H), 7.02 (dd, *J* = 8.2, 2.0 Hz, 1H), 6.81 (d, *J* = 8.2, Hz, 1H), 6.55 (d, *J* = 15.8 Hz, 1H), 3.88 (d, *J* = 5.8 Hz, 2H), 3.82 (s, 3H); ¹³C NMR (DMSO-*d*₆, 125 MHz): δ = 171.9 (COOH), 166.2 (CONH), 148.8, 148.3, 140.0, 126.7, 122.1, 118.8, 116.1, 111.3, 56.0, 41.3; (+)-ESIMS *m/z* 274 ([M + Na]⁺, 100), 525 ([2M + Na]⁺, 63); (-)-ESIMS *m/z* 250 [M-H]⁻.

3.1.2.2. *N*-feruloyl-*L*-alanine (**7**)

White solid (yield % = 92 %); mp 200-201 °C. ¹H NMR (DMSO-*d*₆, 500 MHz): δ = 12.38 (s, OH), 9.45 (s, COOH), 8.24 (d, *J* = 7.4 Hz, 1H, amide-NH), 7.34 (d, *J* = 15.7 Hz, 1H), 7.14 (d, *J* = 2.0 Hz, 1H), 7.01 (dd, *J* = 8.1, 1.9 Hz, 1H), 6.80 (d, *J* = 8.1, Hz, 1H), 6.53 (d, *J* = 15.8 Hz, 1H), 4.33 (p, *J* = 7.2 Hz, 1H), 3.81 (s, 3H), 1.32 (d, *J* = 7.3 Hz, 3H); ¹³C NMR (DMSO-*d*₆, 125 MHz):

$\delta = 174.7$ (COOH), 165.6 (CONH), 148.8, 148.3, 140.0, 126.8, 122.0, 119.0, 116.1, 111.2, 56.0, 48.0, 17.8; (+)-ESIMS m/z 266 ($[M + H]^+$, 42), 280 ($[M + Na]^+$, 56); (-)-ESIMS m/z 264 $[M-H]^-$.

3.1.2.3. *N-feruloyl-L-phenylalanine (8)*

White solid (yield % = 84 %); mp 227-228 °C. 1H NMR (DMSO- d_6 , 500 MHz): $\delta = 12.70$ (s, OH), 9.46 (s, COOH), 8.24 (d, $J = 8.1$ Hz, 1H, amide-NH), 7.31-7.24 (m, 5H), 7.21 (m, 1H), 7.12 (d, $J = 2.0$ Hz, 1H), 6.98 (dd, $J = 8.1, 2.0$ Hz, 1H), 6.79 (d, $J = 8.1$ Hz, 1H), 6.52 (d, $J = 15.7$ Hz, 1H), 4.57 (ddd, $J = 9.4, 8.0, 4.8$ Hz, 1H), 3.81 (s, 3H), 3.12 (dd, $J = 13.9, 4.8$ Hz, 1H), 2.93 (dd, $J = 13.9, 9.5$, 1H); ^{13}C NMR (DMSO- d_6 , 125 MHz): $\delta = 173.6$ (COOH), 165.8 (CONH), 148.8, 148.3, 140.0, 138.1, 129.5, 128.7, 126.9, 126.7, 122.2, 118.8, 116.1, 111.1, 56.0, 54.0, 37.3; (+)-ESIMS m/z 342 ($[M + H]^+$, 5), 364 ($[M + Na]^+$, 100); (-)-ESIMS m/z 341 $[M-H]^-$.

3.1.2.4. *N-feruloyl-L-tyrosine(OBzl) (9)*

White solid (yield % = 76 %); mp 231-232 °C. 1H NMR (DMSO- d_6 , 500 MHz): $\delta = 12.59$ (s, OH), 9.46 (s, COOH), 8.20 (d, $J = 8.2$ Hz, 1H, amide-NH), 7.43 (d, $J = 7.1$ Hz, 2H), 7.38 (d, $J = 7.2$ Hz, 2H), 7.35-7.26 (m, 2H), 7.17 (d, $J = 8.3$ Hz, 2H), 7.13 (d, $J = 1.9$ Hz, 1H), 6.99 (dd, $J = 8.2, 1.9$ Hz, 1H), 6.93 (d, $J = 8.3$ Hz, 2H), 6.80 (d, $J = 8.1$ Hz, 1H), 6.53 (d, $J = 15.7$ Hz, 1H), 5.05 (s, 2H), 4.52 (td, $J = 8.4, 4.7$ Hz, 1H), 3.81 (s, 3H), 3.05 (dd, $J = 14.0, 4.8$ Hz, 1H), 2.86 (dd, $J = 13.9, 9.4$, 1H); ^{13}C NMR (DMSO- d_6 , 125 MHz): $\delta = 173.7$ (COOH), 165.8 (CONH), 157.5, 148.8, 148.3, 140.3, 137.6, 130.5, 130.2, 128.9, 128.2, 128.1, 126.7, 122.2, 118.9, 116.1, 115.0, 111.1, 69.6, 56.0, 54.4, 36.5; (+)-ESIMS m/z 470 $[M + Na]^+$; (-)-ESIMS m/z 446 $[M-H]^-$.

3.1.3. *General procedure for synthesis of N-feruloylamino acid-glycine methyl esters (10-13)*

Compounds (**10-13**) have been synthesized following the same procedure described for compounds (**2-5**). Spectroscopic data of these compounds are listed below.

3.1.3.1. *N-feruloylglycylglycine methyl ester (10)*

White solid (yield % = 86 %); mp 165-167 °C. 1H NMR (DMSO- d_6 , 500 MHz): $\delta = 9.46$ (s, OH), 8.35 (t, $J = 5.9$ Hz, 1H, amide-NH), 8.23 (t, $J = 5.9$ Hz, 1H, amide-NH), 7.35 (d, $J = 15.7$ Hz, 1H), 7.15 (d, $J = 2.0$ Hz, 1H), 7.02 (dd, $J = 8.2, 2.0$ Hz, 1H), 6.80 (d, $J = 8.1$ Hz, 1H), 6.56 (d, $J = 15.7$ Hz, 1H), 3.87 (d, $J = 5.9$ Hz, 4H), 3.81 (s, 3H), 3.64 (s, 3H); ^{13}C NMR (DMSO- d_6 , 125 MHz): $\delta = 170.7$ (COOMe), 170.1 (CONH), 166.2 (CONH), 148.8, 148.3, 139.9, 126.8, 122.0, 119.1,

116.1, 111.3, 56.0, 52.2, 42.4, 41.0; (+)-ESIMS m/z 323 $[M + H]^+$; (-)-ESIMS m/z 321 $[M-H]^-$; (+)-HRESI: $m/z = 323.1236 [M+H]^+$ (calc. 323.1237 for $C_{15}H_{19}N_2O_6$).

3.1.3.2. *N-feruloyl-L-alanylglycine methyl ester (11)*

White solid (yield % = 89 %); mp 103-105 °C. 1H NMR (DMSO- d_6 , 500 MHz): $\delta = 9.45$ (s, OH), 8.37 (t, $J = 5.9$ Hz, 1H, amide-NH), 8.14 (d, $J = 7.8$ Hz, 1H, amide-NH), 7.33 (d, $J = 15.7$ Hz, 1H), 7.13 (d, $J = 2.0$ Hz, 1H), 7.00 (dd, $J = 8.2, 2.0$ Hz, 1H), 6.80 (d, $J = 8.1$ Hz, 1H), 6.58 (d, $J = 15.7$ Hz, 1H), 4.46 (p, $J = 7.2$ Hz, 1H), 3.86 (d, $J = 6.2$ Hz, 2H), 3.81 (s, 3H), 3.63 (s, 3H), 1.27 (d, $J = 7.1$ Hz, 3H); ^{13}C NMR (DMSO- d_6 , 125 MHz): $\delta = 173.4$ (COOMe), 170.7 (CONH), 165.4 (CONH), 148.8, 148.3, 139.7, 126.8, 122.0, 119.3, 116.1, 111.1, 56.0, 52.1, 48.4, 41.0, 18.9; (+)-ESIMS m/z 337 ($[M + H]^+$, 8), 359 ($[M + Na]^+$, 100), 695 ($[2M + Na]^+$, 20); (-)-ESIMS m/z 335 $[M-H]^-$. (+)-HRESI: $m/z = 337.1393 [M+H]^+$ (calc. 337.1394 for $C_{16}H_{21}N_2O_6$).

3.1.3.3. *N-feruloyl-L-phenylalanylglycine methyl ester (12)*

White solid (yield % = 95 %); mp 131-133 °C. 1H NMR (DMSO- d_6 , 500 MHz): $\delta = 9.45$ (s, OH), 8.55 (t, $J = 5.9$ Hz, 1H, amide-NH), 8.20 (d, $J = 8.5$ Hz, 1H, amide-NH), 7.31-7.24 (m, 5H), 7.19 (m, 1H), 7.10 (d, $J = 1.9$ Hz, 1H), 6.97 (dd, $J = 8.2, 1.9$ Hz, 1H), 6.79 (d, $J = 8.1$ Hz, 1H), 6.52 (d, $J = 15.6$ Hz, 1H), 4.71 (ddd, $J = 10.2, 8.5, 4.3$ Hz, 1H), 3.89 (dd, $J = 5.9, 2.7$ Hz, 2H), 3.80 (s, 3H), 3.64 (s, 3H), 3.09 (dd, $J = 13.9, 4.3$ Hz, 1H), 2.82 (dd, $J = 13.9, 10.0$, 1H); ^{13}C NMR (DMSO- d_6 , 125 MHz): $\delta = 172.4$ (COOMe), 170.7 (CONH), 165.7 (CONH), 148.8, 148.2, 139.8, 138.4, 129.6, 128.5, 126.74, 126.72, 122.1, 119.0, 116.1, 111.1, 56.0, 54.0, 52.2, 41.1, 38.2; (+)-ESIMS m/z 435 $[M + Na]^+$; (-)-ESIMS m/z 411 $[M-H]^-$. (+)-HRESI: $m/z = 413.1707 [M+H]^+$ (calc. 413.1707 for $C_{22}H_{25}N_2O_6$).

3.1.3.4. *N-feruloyl-L-tyrosyl(OBzl)glycine methyl ester (13)*

White solid (yield % = 92 %); mp 179-181 °C. 1H NMR (DMSO- d_6 , 500 MHz): $\delta = 9.46$ (s, OH), 8.53 (t, $J = 5.9$ Hz, 1H, amide-NH), 8.16 (d, $J = 8.5$ Hz, 1H, amide-NH), 7.43 (d, $J = 7.1$ Hz, 2H), 7.38 (d, $J = 7.5$ Hz, 2H), 7.32 (m, 1H), 7.26 (d, $J = 15.7$ Hz, 1H), 7.21-7.19 (m, 2H), 7.11 (d, $J = 2.0$ Hz, 1H), 6.98 (dd, $J = 8.2, 2.0$ Hz, 1H), 6.91 (d, $J = 8.3$ Hz, 2H), 6.89 (d, $J = 8.1$ Hz, 1H), 6.53 (d, $J = 15.7$ Hz, 1H), 5.04 (s, 2H), 4.66 (td, $J = 9.2, 4.3$ Hz, 1H), 3.88 (dd, $J = 5.9, 2.6$ Hz, 2H), 3.80 (s, 3H), 3.64 (s, 3H), 3.02 (dd, $J = 14.0, 4.3$ Hz, 1H), 2.75 (dd, $J = 14.0, 9.9$, 1H); ^{13}C NMR (DMSO- d_6 , 125 MHz): $\delta = 172.5$ (COOMe), 170.7 (CONH), 165.6 (CONH), 157.4, 148.8, 148.3,

139.8, 137.6, 130.6, 130.5, 128.8, 128.2, 128.1, 126.7, 122.1, 119.1, 116.1, 114.8, 111.1, 69.6, 56.0, 54.5, 52.2, 41.1, 37.4; (+)-ESIMS m/z 541 $[M + Na]^+$; (-)-ESIMS m/z 517 $[M-H]^-$; (+)-HRESI: $m/z = 519.2131$ $[M+H]^+$ (calc. 519.2126 for $C_{29}H_{31}N_2O_7$).

3.1.4. General procedure for synthesis of *N*-feruloylamino acid-glycine methyl esters (**14-17**)

Synthesis of compounds (**14-17**) has been accomplished using the same method described for compounds (**2-5**). Spectroscopic data of these compounds are listed below.

3.1.4.1. *N*-feruloylglycyl-*L*-alanine methyl ester (**14**)

White solid (yield % = 87 %); mp 161-163 °C. 1H NMR (DMSO- d_6 , 500 MHz): $\delta = 9.45$ (s, OH), 8.38 (d, $J = 7.1$ Hz, 1H, amide-NH), 8.14 (t, $J = 5.8$ Hz, 1H, amide-NH), 7.34 (d, $J = 15.6$ Hz, 1H), 7.15 (d, $J = 1.9$ Hz, 1H), 7.01 (dd, $J = 8.2, 1.9$ Hz, 1H), 6.80 (d, $J = 8.1$ Hz, 1H), 6.57 (d, $J = 15.7$ Hz, 1H), 4.31 (p, $J = 7.2$ Hz, 1H), 3.87 (dd, $J = 12.6, 5.8$ Hz, 2H), 3.81 (s, 3H), 3.63 (s, 3H), 1.29 (d, $J = 7.3$ Hz, 3H); ^{13}C NMR (DMSO- d_6 , 125 MHz): $\delta = 173.4$ (COOMe), 169.3 (CONH), 166.1 (CONH), 148.8, 148.3, 139.8, 126.8, 122.0, 119.1, 116.1, 111.3, 56.0, 52.3, 48.0, 42.2, 17.5; (+)-ESIMS m/z 337 ($[M + H]^+$, 4), 359 ($[M + Na]^+$, 100), 695 ($[2M + Na]^+$, 32); (+)-HRESI: $m/z = 337.1398$ $[M+H]^+$ (calc. 337.1394 for $C_{16}H_{21}N_2O_6$).

3.1.4.2. *N*-feruloyl-*L*-alanyl-*L*-alanine methyl ester (**15**)

White solid (yield % = 89 %); mp 109-111 °C. 1H NMR (DMSO- d_6 , 500 MHz): $\delta = 9.44$ (s, OH), 8.39 (d, $J = 7.0$ Hz, 1H, amide-NH), 8.08 (d, $J = 7.8$ Hz, 1H, amide-NH), 7.32 (d, $J = 15.6$ Hz, 1H), 7.13 (d, $J = 2.0$ Hz, 1H), 6.99 (dd, $J = 8.2, 2.0$ Hz, 1H), 6.80 (d, $J = 8.1$ Hz, 1H), 6.58 (d, $J = 15.7$ Hz, 1H), 4.46 (p, $J = 7.2$ Hz, 1H), 4.28 (p, $J = 7.1$ Hz, 1H), 3.81 (s, 3H), 3.63 (s, 3H), 1.30 (d, $J = 7.3$ Hz, 3H), 1.25 (d, $J = 7.1$ Hz, 3H); ^{13}C NMR (DMSO- d_6 , 125 MHz): $\delta = 173.4$ (COOMe), 172.8 (CONH), 165.4 (CONH), 148.8, 148.3, 139.7, 126.8, 122.0, 119.3, 116.1, 111.1, 56.0, 52.3, 48.2, 48.0, 18.9, 17.3; (+)-ESIMS m/z 351 ($[M + H]^+$, 6), 373 ($[M + Na]^+$, 100), 723 ($[M + 2Na]^+$, 15); (+)-HRESI: $m/z = 351.1554$ $[M+H]^+$ (calc. 351.1551 for $C_{17}H_{23}N_2O_6$).

3.1.4.3. *N*-feruloyl-*L*-phenylalanyl-*L*-alanine methyl ester (**16**)

White solid (yield % = 96 %); mp 123-125 °C. 1H NMR (DMSO- d_6 , 500 MHz): $\delta = 9.44$ (s, OH), 8.58 (d, $J = 7.1$ Hz, 1H, amide-NH), 8.14 (d, $J = 8.6$ Hz, 1H, amide-NH), 7.32-7.24 (m, 5H), 7.19 (m, 1H), 7.10 (d, $J = 1.9$ Hz, 1H), 6.97 (dd, $J = 8.2, 2.0$ Hz, 1H), 6.78 (d, $J = 8.1$ Hz, 1H), 6.51 (d,

$J = 15.7$ Hz, 1H), 4.71 (ddd, $J = 9.4, 8.0, 4.8$ Hz, 1H), 4.31 (p, $J = 7.1$ Hz, 1H), 3.80 (s, 3H), 3.63 (s, 3H), 3.07 (dd, $J = 14.0, 4.1$ Hz, 1H), 2.80 (dd, $J = 13.9, 9.5$, 1H), 1.32 (d, $J = 7.3$ Hz, 3H); ^{13}C NMR (DMSO- d_6 , 125 MHz): $\delta = 173.4$ (COOMe), 171.9 (CONH), 165.6 (CONH), 148.8, 148.2, 139.8, 138.2, 129.6, 128.5, 126.74, 126.70, 122.1, 119.1, 116.1, 111.1, 56.0, 54.0, 52.4, 48.0, 38.2, 17.4; (+)-ESIMS m/z 427 ($[\text{M} + \text{H}]^+$, 5), 449 ($[\text{M} + \text{Na}]^+$, 100); (+)-HRESI: $m/z = 427.1865$ $[\text{M} + \text{H}]^+$ (calc. 427.1864 for $\text{C}_{23}\text{H}_{27}\text{N}_2\text{O}_6$).

3.1.4.4. *N-feruloyl-L-tyrosyl(OBzl)-L-alanine methyl ester (17)*

White solid (yield % = 91 %); mp 180-182 °C. ^1H NMR (DMSO- d_6 , 500 MHz): $\delta = 9.45$ (s, OH), 8.56 (d, $J = 7.1$ Hz, 1H, amide-NH), 8.10 (d, $J = 8.6$ Hz, 1H, amide-NH), 7.43 (d, $J = 7.1$ Hz, 2H), 7.38 (d, $J = 7.2$ Hz, 2H), 7.34-7.29 (m, 1H), 7.25 (d, $J = 15.7$ Hz, 1H), 7.21 (d, $J = 8.6$ Hz, 2H), 7.11 (d, $J = 2.0$ Hz, 1H), 6.97 (dd, $J = 8.2, 2.0$ Hz, 1H), 6.91 (d, $J = 8.3$ Hz, 2H), 6.79 (d, $J = 8.1$ Hz, 1H), 6.52 (d, $J = 15.7$ Hz, 1H), 5.05 (s, 2H), 4.66 (td, $J = 8.4, 4.7$ Hz, 1H), 4.30 (p, $J = 7.2$ Hz, 1H), 3.81 (s, 3H), 3.63 (s, 3H), 3.00 (dd, $J = 14.1, 4.1$ Hz, 1H), 2.73 (dd, $J = 14.2, 9.9$ Hz, 1H), 1.32 (d, $J = 7.3$ Hz, 3H); ^{13}C NMR (DMSO- d_6 , 125 MHz): $\delta = 173.4$ (COOMe), 171.9 (CONH), 165.6 (CONH), 157.4, 148.8, 148.3, 139.8, 137.6, 130.65, 130.6, 128.8, 128.14, 128.11, 126.8, 122.1, 119.1, 116.1, 114.8, 111.1, 69.6, 56.0, 54.3, 52.3, 48.0, 37.4, 17.4; (+)-ESIMS m/z 533 ($[\text{M} + \text{H}]^+$, 2), 555 ($[\text{M} + \text{Na}]^+$, 100); (+)-HRESI: $m/z = 533.2286$ $[\text{M} + \text{H}]^+$ (calc. 533.2282 for $\text{C}_{30}\text{H}_{33}\text{N}_2\text{O}_7$).

3.2. *Antibacterial Activity assay*

Antibacterial activity testing of the synthesized compounds was carried out against a set of bacterial strains using paper-disk diffusion assay [37] with some modifications according to our previous work [33].

3.3. *Cell Lines*

Cell lines were purchased from the American Type Culture Collection (ATCC, Rockville, MD) or German Collection of Microorganisms and Cell Cultures (DSMZ, Braunschweig, Germany) and cultured as recommended by suppliers.

3.4. *Cell Viability Analysis*

The XTT cell viability assay (Roche Diagnostics, Filderstadt, Germany) is a colorimetric assay that measures cellular metabolic activity. The assay is based on the mitochondrial reduction of tetrazolium salt by viable cells with active mitochondrial dehydrogenase into the orange colored water-soluble formazan salt. Different types of cancer cells were plated in 96-well microtiter plates and treated with different concentrations of the respective compounds for 48 h before incubating with XTT labeling mixture at 37 °C [38-40]. The spectrophotometric absorbance was measured using a TECAN Infinite® 200 PRO microplate reader (Männedorf, Switzerland) at 450 nm with a 630 nm-reference filter. Paclitaxel (MP Biomedicals, Santa Ana, CA) served as a positive control.

3.5. *Caspase-Glo® 3/7 Assay*

The Caspase-Glo® 3/7 assay (Promega, Madison, WI, USA) is a lytic luminogenic assay that measures caspase-3 and 7 activities. The assay provides a luminogenic caspase-3/7 substrate, which contains the tetrapeptide sequence DEVD (Z-DEVD-aminoluciferin), in a reagent optimized for caspase activity, luciferase activity and cell lysis. The liberated aminoluciferin serves as a substrate for luciferase to produce measurable light emission equivalent to caspase 3 and 7 activities. Briefly, the triple-negative MDA-MB-231 breast cancer cells were treated with either ferulic acid, its synthesized derivatives at concentrations of 10 and 30 µM, paclitaxel (100 nM), or doxorubicin (100 nM) for 24 and 48 h, and the activity of caspase 3/7 was assessed using a Caspase-Glo® 3/7 activity kit according to the manufacturer's instructions.

3.6. *Analysis of Mitochondrial Integrity*

The triple-negative MDA-MB-231 breast cancer cells were treated with either ferulic acid, or its synthesized derivatives at a concentration of 10 µM, doxorubicin (100 nM), or paclitaxel (100 nM) for 24 h. The voltage-sensitive lipophilic cationic probe, JC-1 sensor (Molecular Probes, San Diego, CA, USA) concentrates selectively in the energized mitochondria to form red fluorescent aggregates at 590 nm in response to their higher membrane potential. By contrast, the monomeric form of the dye dispersed into the cytosol of the cells upon leakage from deenergized mitochondria emits green fluorescence at 527 nm. The treated cells were loaded with 10 µg/ml JC-1 dye in serum-free medium for 20 min at 37 °C [38,39] and analyzed by flow cytometry (FACS Verse, BD Biosciences, San Jose, CA, USA). MDA-MB-231 cells treated with the mitochondrial uncoupler FCCP (50 µM, 2 h) served as positive control (Sigma, St. Louis, MO, USA).

3.7. *Human Tumor Xenografts as Preclinical in Vivo Model*

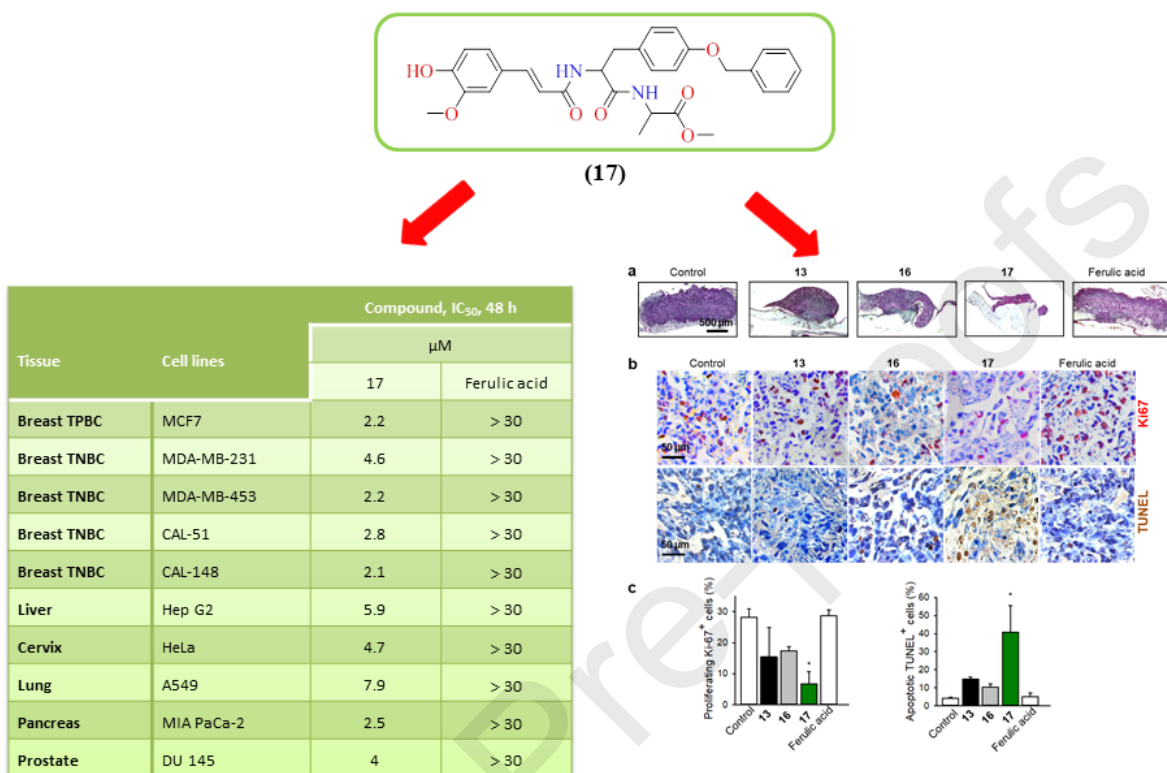
The triple-negative MDA-MB-231 breast cancer cells were xenotransplanted onto the chick chorioallantoic membrane 8 days after fertilization. The next day, the xenografts were topically treated for 3 consecutive days with 20 μ l of either ferulic acid, or its synthesized derivatives at a concentration of 10 μ M. On day 12 after fertilization, the xenografts were collected, fixed, and paraffin-embedded for histological analysis. Serial sections (5 μ m) were stained for the human proliferation antigen Ki-67 using a specific antibody from DakoCytomation (Glostrup, Denmark). For the detection of apoptotic cells, DNA strand breaks were visualized by the terminal deoxynucleotidyl transferase dUTP nick-end labeling (TUNEL) method using a TUNEL assay kit (Roche Diagnostics) [38]. The sections were counterstained with hematoxylin and images were digitally recorded with an Axio Lab.A1 microscope (Carl Zeiss, Göttingen, Germany) and a Zeiss 2/3" CMOS camera using Progres Gryphax software (Carl Zeiss, Göttingen, Germany). The study protocol complies with the Guide for the Care and Use of Laboratory Animals issued by US and European regulatory agencies. Avian embryos in this study were sacrificed prior to 7 days before hatching.

3.8. *Statistical Analysis*

All values are expressed as mean \pm standard error of the mean (SEM). Statistical analysis was performed using the Newman-Keuls post-hoc test for multigroup comparisons by using Sigmaplot 14.0 (Systat Software Inc., San Jose, CA, USA).

Acknowledgments: The authors are grateful to the NMR and MS Departments at Bielefeld University for the spectral measurements. We would like to thank Carmela Michalek for the *in vitro* analysis of KB-3-1 cell line, Marco Wißbrock and Anke Nieß for technical assistance. This research work has been financed by DAAD in the frame of the Research Project ID 57166072 and by the Academic Center for Complementary and Integrative Medicine (AZKIM), State Ministry of Baden-Württemberg for Sciences, Research and Arts.

Graphical abstract



Highlights

- A novel series of feruloyl dipeptide derivatives were synthesized and their anticancer activity was evaluated.
- Feruloyl dipeptides with aromatic amino acid residues (**12**, **13**, **16**, **17**) were the most potent and **17** showed to be the best active anticancer agents.
- Compound **17** induced a strong mitochondrial transmembrane potential dissipation.
- Compound **17** induced activation of caspase 3/7 in the triple-negative MDA-MB-231 breast cancer cell line.
- Compound **17** induced apoptosis and inhibited growth of the triple-negative MDA-MB-231 breast cancer xenografts *in vivo*.

Declaration of interests

The authors declare that they have no known competing financial interests or personal relationships that could have appeared to influence the work reported in this paper.

The authors declare the following financial interests/personal relationships which may be considered as potential competing interests:

References

- [1] R.L. Siegel, K.D. Miller, A. Jemal, Cancer statistics, 2018, *CA Cancer J. Clin.*, 68 (2018) 7-30.
- [2] L.A. Torre, F. Bray, R.L. Siegel, J. Ferlay, J. Lortet-Tieulent, A. Jemal, Global cancer statistics, 2012, *CA Cancer J. Clin.*, 65 (2015) 87-108.
- [3] L. Carey, E. Winer, G. Viale, D. Cameron, L. Gianni, Triple-negative breast cancer: disease entity or title of convenience? *Nat. Rev. Clin. Oncol.*, 7 (2010) 683-692.
- [4] E. Lee, R. McKean-Cowdin, H. Ma, D.V. Spicer, D. Van Den Berg, L. Bernstein, G. Ursin, Characteristics of triple-negative breast cancer in patients with a BRCA1 mutation: results from a population-based study of young women, *J. Clin. Oncol.*, 29 (2011) 4373-4380.
- [5] J.H. Park, J.H. Ahn, S.B. Kim, How shall we treat early triple-negative breast cancer (TNBC): from the current standard to upcoming immuno-molecular strategies. *ESMO Open*, 3 (2018) e000357.
- [6] C.R. Santangelo, Ferulic acid: pharmacological and toxicological aspects, *Food Chem. Toxicol.*, 65 (2014)185-195.
- [7] S. Westfall, N. Lomis, S.P. Singh, S.Y. Dai, S. Prakash, The Gut Microflora and its Metabolites Regulate the Molecular Crosstalk between Diabetes and Neurodegeneration, *J. Diabetes Metab.*, 6 (2015) 577.
- [8] Z. Zhao, M.H. Moghadasian, Chemistry, natural sources, dietary intake and pharmacokinetic properties of ferulic acid: A review, *Food Chem.*, 109 (2008) 691-702.
- [9] K.Yama, T.B.T. Lam, B.A. Stone, Covalent cross-links in the cell wall, *Plant Physiol.*, 104 (1994) 315-320.
- [10] K. Rumbold, P. Biely, M. Mastihubova, J. Gudel, G. Gubitz, K.H. Robra, B.A. Prior, Purification and properties of a feruloyl esterase involved in lignocellulose degradation by *Aureobasidium pullulans*, *Appl. Environ. Microbiol.*, 69 (2003) 5622-5626.
- [11] A.E. Fazary, Y.H. JU, Feruloyl esterases as biotechnological tools: current and future perspectives, *Acta Biochim. Biophys. Sin.*, 39 (2007) 811-828.

- [12] S. Ou, K.C. Kwok, Ferulic acid: pharmaceutical functions, preparation and applications in foods, *J. Sci. Food Agric.*, 84 (2004) 1261-1269.
- [13] S. Itagaki, T. Kurokawa, C. Nakata, Y. Saito, S. Oikawa, M. Kobayashi, In vitro and in vivo antioxidant properties of ferulic acid: a comparative study with other natural oxidation inhibitors, *Food Chem.*, 114 (2009) 466-471.
- [14] L.B.d. Paiva, R. Goldbeck, W.D.d. Santos, F.M. Squina, Ferulic acid and derivatives: molecules with potential application in the pharmaceutical field, *Braz. J. Pharm. Sci.*, 49 (2013) 395-411.
- [15] M. Hirose, S. Takahashi, K. Ogawa, M. Futakuchi, T. Shirai, Phenolics: blocking agents for heterocyclic amine-induced carcinogenesis, *Food Chem. Toxicol.*, 37 (1999) 985-992.
- [16] M.S. Balasubashini, R. Rukkumani, P. Viswanathan, V.P. Menon, Ferulic acid alleviates lipid peroxidation in diabetic rats, *Phytother. Res.*, 18 (2004) 310-314.
- [17] R. Rukkumani, K. Aruna, P.S. Varma, V.P. Menon, Influence of ferulic acid on circulatory prooxidant-antioxidant status during alcohol and PUFA induced toxicity, *J. Physiol. Pharmacol.*, 55 (2004) 551-561.
- [18] T.S. Shanmugarajan, E. Krishnakumar, I. Somasundaram, D. Sivaraman, M. Arunsundar, R. Balaji, S.M. Sivakumar, Salutary effect of ferulic acid against D-galactosamine challenged liver damage, *J. Biol. Sci.*, 8 (2008) 1271-1279.
- [19] M. Srinivasan, R. Rukkumani, A. Ramsudheer, V.P. Menon, Ferulic acid, a natural protector against carbon tetrachloride induced toxicity, *Fundam. Clin. Pharmacol.*, 19 (2005) 491-496.
- [20] M. Edeas, Y. Khalfoun, Y. Lazizi, L. Vergne, S. Labidalle, E. Postaire, A. Lindenbaum, Effect of the liposolubility of free radical scavengers on the production of antigen P24 from a HIV infected monocytic cell line, *C R Seances Soc. Biol. Fil.*, 189 (1995) 367-373.
- [21] Y.C. Jeong, H.M. Jae, H.P. Keun, Isolation and identification of 3-methoxy-4-hydroxybenzoic acid and 3-methoxy-4-hydroxycinnamic acid from hot water extracts of

- Hovenia dulcis Thumb and confirmation of their antioxidative and antimicrobial activity, Korean J. Food Sci. Technol., 32 (2000) 1403-1408.
- [22] T. Hirabayashi, H. Ochiai, S. Sakai, K. Nakajima, K. Terasawa, Inhibitory effect of ferulic acid and isoferulic acid on murine interleukin-8 production in response to influenza virus infections in-vitro and in-vivo, Planta Med., 61 (1995) 221-226.
- [23] H.K. Kim, T.S. Jeong, M.K. Lee, Y.B. Park, M.S. Choi, Lipid lowering efficacy of hesperidin metabolites in high-cholesterol fed rats, Clin. Chim. Acta, 327 (2003)129-137.
- [24] J. Kanski, M. Aksenova, A. Stoyanova, D.A. Butterfield, Ferulic acid antioxidant protection against hydroxyl and peroxy radical oxidation in synaptosomal and neuronal cell culture systems in vitro: structure activity studies, J. Nutr. Biochem., 13 (2002) 273-281.
- [25] A. Saija, A. Tomaino, D. Trombetta, A. De Pasquale, N. Uccella, T. Barbuzz, D. Paolino, F. Bonina, In vitro and in vivo evaluation of caffeic and ferulic acids as topical photoprotective agents, Int. J. Pharm., 199 (2000) 39-47.
- [26] O.I. Aruoma, M.J. Laughton, B. Halliwell, Carnosine, homocarnosine and anserine: could they act as antioxidants in vivo? Biochem. J., 264 (1989) 863-869.
- [27] T. Goto, D. Ishii, Y. Enomoto-Rogers, A. Takemura, T. Iwata, Synthesis and characterization of poly[(ferulic acid)-alt-(glycine)], Polymer, 112 (2017) 385-392.
- [28] B.I. Roman, J-C. Monbaliu, L.M. De Coen, S. Verhasselt, B. Schuddinck, E. Van Hoeylandt, C.V. Stevens, Feruloylbenzotriazole and Weinreb amide as bioinspired building blocks: A reactivity study towards O-,N-,S-, and C-nucleophiles, Eur. J. Org. Chem., 2014 (2014) 2594-2611.
- [29] V.D. Kancheva, Phenolic antioxidants, radical-scavenging and chain-breaking activity: A comparative study, Eur. J. Lipid Sci. Technol., 111 (2009) 1072-1089.
- [30] X-L. Hu, J. Lin, X-Y. Lv, J-H. Feng, X-Q. Zhang, H. Wang, W-C. Ye, Synthesis and biological evaluation of clovamide analogues as potent anti-neuroinflammatory agents in vitro and in vivo, Eur. J. Med. Chem., 151 (2018) 261-271.

- [31] B. Shi, L. Yang, T. Gao, C. Ma, Q. Li, Y. Nan, S. Wang, C. Xiao, P. Jia, X. Zheng, Pharmacokinetic profile and metabolite identification of bornyl caffeate and caffeic acid in rats by high performance liquid chromatography coupled with mass spectrometry, *RSC Adv.*, 9 (2019) 4015-4027.
- [32] B.N. Sudha, N. Yellasubbaiah, K. Bharathi, Synthesis, characterization and biochemical evaluation of N-[3-(substituted phenyl)-1-oxo-2-propenyl]alanine, *Int. J. Chem. Sci.*, 13 (2015) 837-848.
- [33] A. Hamed, A.S. Abdel-Razek, M. Frese, J. Sproß, H-G. Stammer, N. Sewald, M. Shaaban, Coumamarin: a first coumarinyl calcium complex isolated from nature, *J. Antibiot.*, 72 (2019) 729–735.
- [34] N. Nasr Bouzaiene, S. Kilani Jaziri, H. Kovacic, L. Chekir-Ghedira, K. Ghedira, J. Luis, The effects of caffeic, coumaric and ferulic acids on proliferation, superoxide production, adhesion and migration of human tumor cells in vitro, *Eur. J. Pharmacol.*, 766 (2015) 99-105.
- [35] C. Wang, R.J. Youle, The role of mitochondria in apoptosis, *Annu. Rev. Genet.*, 43 (2009) 95-118.
- [36] S.L. Fink, B.T. Cookson, Apoptosis, pyroptosis, and necrosis: mechanistic description of dead and dying eukaryotic cells, *Infect. Immun.*, 73 (2005) 1907-1916.
- [37] A.W. Bauer, W.M. Kirby, J.C. Sherris, M. Truck, Antibiotic susceptibility testing by a standardized single disk method, *Am. J. Clin. Pathol.*, 45 (1966) 493-496.
- [38] M. El Gaafary, B. Büchele, T. Syrovets, S. Agnolet, B. Schneider, C.Q. Schmidt, T. Simmet, An α -acetoxy-tirucallic acid isomer inhibits Akt/mTOR signaling and induces oxidative stress in prostate cancer cells, *J. Pharmacol. Exp. Ther.*, 352 (2015) 33-42.
- [39] M. El Gaafary, S.M. Ezzat, A.M. El Sayed, O.M. Sabry, S. Hafner, S. Lang, M. Schmiech, T. Syrovets, T. Simmet, Acovenoside A induces mitotic catastrophe followed by apoptosis in non-small-cell lung cancer cells, *J. Nat. Prod.*, 80 (2017) 3203-3210.
- [40] C. Schmidt, C. Loos, L. Jin, M. Schmiech, C.Q. Schmidt, M.E. Gaafary, T. Syrovets, T. Simmet, Acetyl-lupeolic acid inhibits Akt signaling and induces apoptosis in

chemoresistant prostate cancer cells *in vitro* and *in vivo*, *Oncotarget*, 8 (2017) 55147-55161.

Journal Pre-proofs